

ELECTROREFINING URANIUM

An Undergraduate Research Scholars Thesis

by

SAMUEL S. OLIVIER

Submitted to the Undergraduate Research Scholars program
Texas A&M University
in partial fulfillment of the requirements for the designation as an

UNDERGRADUATE RESEARCH SCHOLAR

Approved by
Research Advisor:

Dr. Sean McDeavitt

May 2016

Major: Nuclear Engineering

TABLE OF CONTENTS

	Page
ABSTRACT	1
DEDICATION	2
ACKNOWLEDGMENTS	3
NOMENCLATURE	4
I INTRODUCTION	5
Objectives	6
II BACKGROUND	8
Properties of uranium	8
Electrolysis	10
III LITERATURE REVIEW	16
Los Alamos National Laboratory	16
Argonne National Laboratory	17
Idaho National Laboratory	23
IV EXPERIMENTAL SETUP	25
Glove box	25
Heater well	27
Refiner crucible	32
Electrorefining process	33
V LIST OF DEVICES	34
VI FUTURE WORK	35
REFERENCES	36

ABSTRACT

Electrorefining Uranium

Samuel S. Olivier
Department of Nuclear Engineering
Texas A&M University

Research Advisor: Dr. Sean McDevitt
Department of Nuclear Engineering

The Fuel Cycle and Materials Laboratory at Texas A&M University needs a method of removing impurities from depleted uranium samples. A non-aqueous, lab-scale electrorefiner will be constructed to solve this problem. The electrorefiner will employ electrolysis to electrochemically separate the uranium from the impurities in the samples. Electrorefining has been applied to reprocessing spent nuclear fuel and is an effective way to close the nuclear fuel cycle. Los Alamos National Laboratory, Argonne National Laboratory and Idaho National Laboratory have conducted extensive research on electrorefining spent nuclear fuel. This report contains a discussion on the importance and theoretical background of electrorefining, a literature review of previous work conducted by Los Alamos National Laboratory, Argonne National Laboratory and Idaho National Laboratory and the design of the lab-scale electrorefiner to be built at the Fuel Cycle and Materials Laboratory.

DEDICATION

I dedicate this research to my parents, Steve and Maryle Olivier, for without their love and support this project would not have been possible.

ACKNOWLEDGMENTS

I would like to thank Dr. Sean McDevitt for providing me with this excellent opportunity to further my education and for his guidance and support throughout this project. I would also like to extend my gratitude to Dr. Luis Ortega, Dr. Delia Perez and Brandon Blamer for their help in the completion of this project and the writing of this thesis.

NOMENCLATURE

ANL Argonne National Laboratory

CE current efficiency

DU depleted uranium

EBR-II Experimental Breeder Reactor II

ER electrorefiner

FCML Fuel Cycle and Materials Laboratory

FDB Fuel Dissolution Basket

IFR Integral Fast Reactor

INL Idaho National Laboratory

LANL Los Alamos National Laboratory

MOX Mixed Oxide Fuel

MSR Molten Salt Reactor

MSRE Molten Salt Reactor Experiment

PUREX Plutonium Uranium Extraction

SNF spent nuclear fuel

CHAPTER I

INTRODUCTION

Spent nuclear fuel (SNF) from a typical, commercial reactor, while de-enriched and no longer useful in a thermal reactor in its current form, still contains a high level of usable fuel in the form of unburnt ^{235}U , fertile ^{238}U and fissile plutonium. The rest of the SNF is nuclear waste from fission products of which the minor actinides are the most important due to their high radioactivity and long half-life. Reprocessing seeks to extract the useful elements of SNF for reuse in an effort to increase fuel utilization and reduce waste volume. Reducing the concentration of plutonium in spent fuel also increases nuclear security [1].

Recycled fuel can be re-enriched to make use of the remaining fissile uranium or separated to make use of the plutonium content of SNF. Separation of plutonium is primarily achieved through a hydrometallurgical process known as the Plutonium Uranium Extraction (PUREX) process. The separated plutonium is used to create Mixed Oxide Fuel (MOX) which relies on higher plutonium concentration to counterbalance lower enrichments of uranium [2]. MOX fuel can be used as an alternative to low enriched uranium in a thermal reactor.

PUREX was originally designed as a method for producing weapons grade plutonium during World War II and has come under scrutiny as a nuclear safety issue due to its production of separate streams of high concentration uranium and plutonium. The separate streams are later blended down to lower, less dangerous levels [3]. However, the intermediate, high concentration step in the process presents an unnecessary nuclear security risk. The PUREX process and its derivatives also leave behind minor actinides resulting in longer lived and more active waste [1].

An alternative to PUREX is electrorefining which is often called pyroprocessing due to the high temperatures involved. The name electrorefining came about due to the considerable purification of SNF obtained [4]. Electrorefining uses electric current to separate metals and avoids creating free streams of uranium, plutonium and waste by co-collecting uranium, plutonium and most other actinides simultaneously. The resulting recycled fuel is a highly radioactive, actinide mixture. The mixture's radioactivity and the dilution of plutonium increases the difficulty of theft and non-

peaceful use. As more of the minor actinides are collected, the resulting waste is shorter lived and safer to handle. The co-collected fuel not only results in less nuclear waste but is also readily usable in a fast reactor [1].

Fast reactors can make use of all of the actinides whereas thermal reactors primarily use only the fissile and fertile actinides. This means that all of the co-collected fuel can be used in a fast reactor in breeding reactions or fission. Due to the burnup of the actinides, the resulting waste from fast reactors is much shorter lived and less radioactive than a thermal reactor's waste [5]. In addition, by surrounding the reactor with a ^{238}U blanket, fast reactors can produce MOX fuel.

Many fast reactor designs, such as the Integral Fast Reactor (IFR) and Molten Salt Reactor (MSR), depend on on-site pyroprocessing. Pyroprocessing syncs well with the fast reactor fuel cycle because the high temperatures involved with pyroprocessing allows the fuel to be processed without cooling [1]. On-site processing eliminates the security risk of transporting nuclear material as well [6].

Pyroprocessing serves as a promising alternative to hydrometallurgical methods of reprocessing spent fuel and is an effective way to close the nuclear fuel cycle. Similar processes have already been commercialized for the purification of copper and the electroplating of nickel. Electrorefining has been extensively researched by Los Alamos National Lab, Argonne National Lab and Idaho National Lab.

Objectives

The Fuel Cycle and Materials Laboratory at Texas A&M University currently needs a method of removing impurities from depleted uranium samples. Impure samples increase the difficulty of experimentation and can lead to inaccurate data and incorrect conclusions. A non-aqueous, lab scale electrorefining system will be constructed to solve this problem.

The objective of this project is to design, fabricate and operate a molten salt electrorefiner to purify depleted uranium samples. This project will focus on efficiently purifying uranium by extending the knowledge of electrolysis to uranium metal and applying the processes and techniques used in reprocessing spent fuel. In addition, it will provide the Fuel Cycle and Materials Laboratory

the capability to purify uranium in the lab. This paper will discuss the background, history and theory of electrorefining and present the equipment designs and methods of construction of the the electrorefiner.

CHAPTER II

BACKGROUND

Properties of uranium

Radiological properties

Uranium occurs in nature as a mixture of ^{238}U , ^{235}U and ^{234}U [7]. The natural abundances of each isotope are 99.275% ^{238}U , 0.720% ^{235}U and 0.005% ^{234}U [8]. The uranium metal used in this experiment is depleted uranium (DU) which has lower than natural levels of ^{235}U . DU therefore consists primarily of ^{238}U with negligible amounts of ^{234}U and ^{235}U .

^{238}U decays through alpha emission and is not very radioactive due to its long half-life of 4.5 billion years. In addition, alpha particles have a short range in tissue and are thus only a hazard when internalized [10]. ^{238}U begins the uranium series which ends with stable ^{206}Pb [11]. Figure II.1 shows the order of the nuclides in the uranium series, their decay type and their half-life.

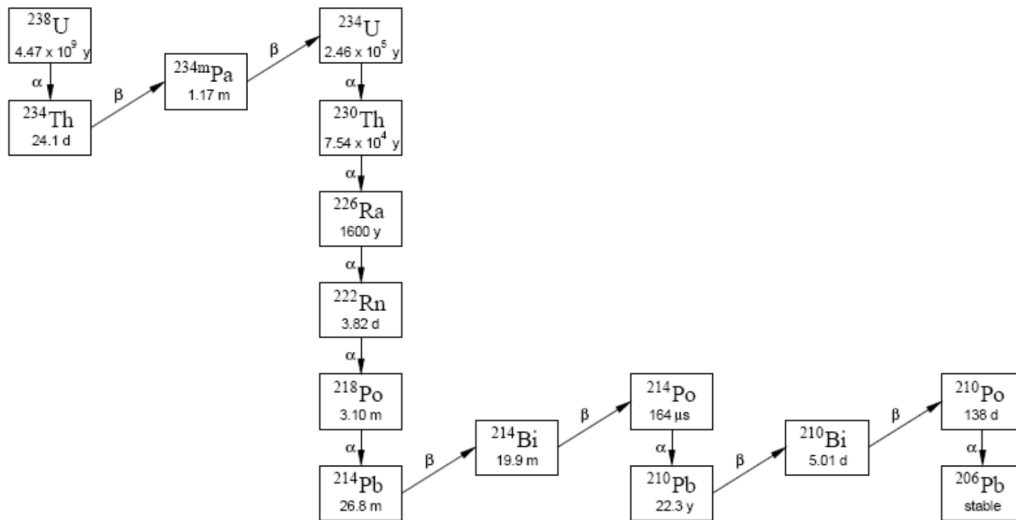


Fig. II.1.: A schematic of the order of decay, decay type and half-lives of the uranium series. Due to the composition of depleted uranium samples, decays are expected to follow this chain [9].

Notable nuclides within this decay chain are ^{234}Th and ^{234m}Pa . These nuclides are beta and gamma emitters with half-lives of 24.1 days and 1.175 minutes [12].

While initially DU only emits alpha particles, as it decays, gamma and beta emitters and more active nuclides emerge. The activity of 1 kg of initially pure ^{238}U is plotted in Figure II.2. Figure II.2 shows that after 6 months the activities of ^{238}U , ^{234}Th and ^{234m}Pa are equal. Thus one can expect 2 beta emissions for every 1 alpha emission from DU after 6 months of decay [12].

The total activity exponentially increases during the first 6 months and then levels out as secular equilibrium between ^{238}U , ^{234}Th and ^{234m}Pa is reached [13]. The flat slope in total activity is due to the long half-lives of ^{234}U and ^{230}Th which serve to slow the progression through the uranium series [12].

The emission of beta particles and gamma rays from ^{234}Th , ^{234m}Pa and ^{234}Pa present an external hazard while the alpha decay of ^{238}U is an internal hazard [11]. Thus, all DU samples must be handled appropriately.

Chemical properties

The element uranium can exist in five oxidation states: +2, +3, +4, +5 and +6, however, only uranium(VI) and uranium(IV) are stable enough to be of practical importance [15]. Uranium typically appears in oxidation states of +6 and +4 and is strongly electropositive and reactive [7]. Finely divided uranium metal is pyrophoric when exposed to oxygen and is reactive with all the components of the atmosphere except the noble gases even at room temperature [16]. Oxidation of uranium metal in dry air produces an adherent UO_2 layer at low temperature and a U_3O_8 layer at higher temperatures [7]. To avoid ignition and oxygen contamination, DU samples will be handled in an argon filled glove box.

Uranium metal is inert to alkali metals such as lithium, sodium and potassium [7]. Thus solvent solutions containing alkali metals are preferred to prevent side reactions with uranium.

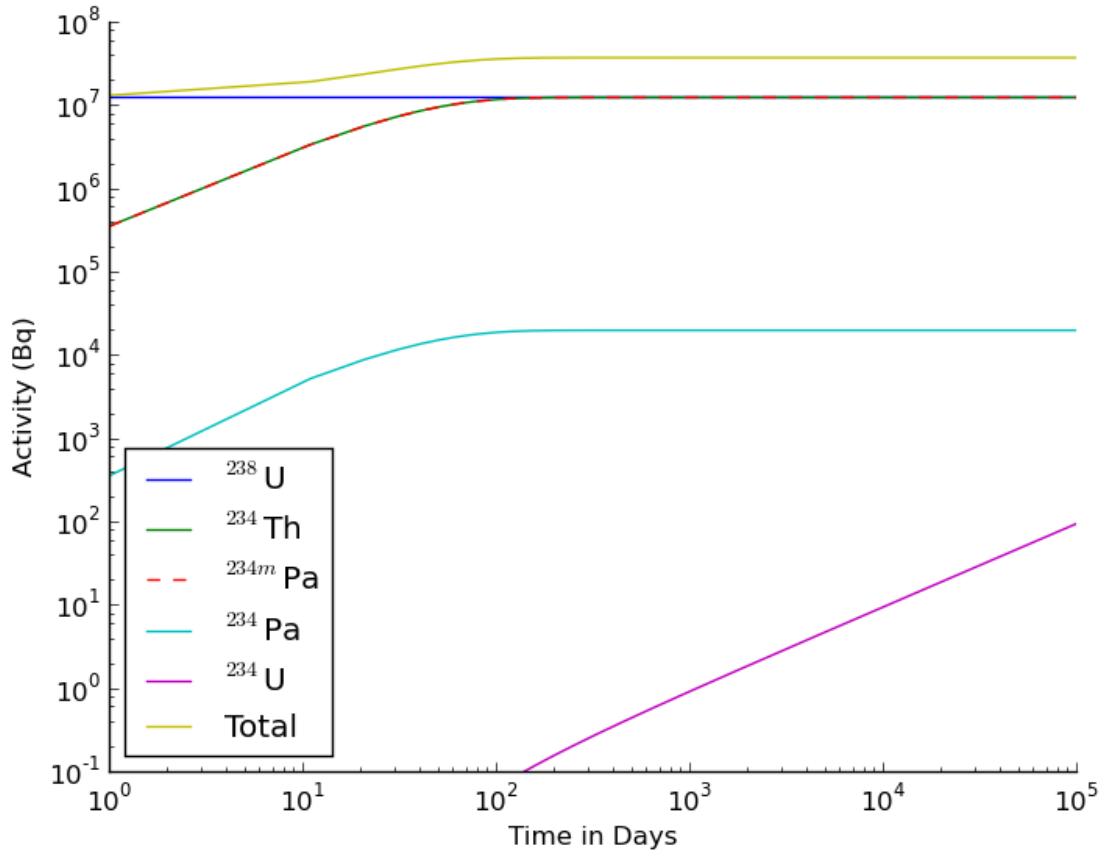


Fig. II.2.: A plot of the activities of ^{238}U , ^{234}Th , ^{234m}Pa , ^{234}Pa and ^{234}U versus time from a 1 kg, initially pure sample of ^{238}U . Secular equilibrium between ^{238}U , ^{234}Th and ^{234m}Pa is reached at around 180 days (6 months). The total activity reaches an approximately constant value after this time due to the long half-lives of ^{234}U and ^{230}Th . This plot was generated using the decay kinetics equations from [13]. Half-life values were taken from [14].

Electrolysis

Electrorefining is the process of metal electrodeposition through electrolysis and is often called pyroprocessing due to the high temperatures involved [1]. Electrorefining has been used extensively for commercial purification of metals in aqueous solutions such as copper, nickel, cobalt, lead, tin, silver and gold. Molten salt electrorefining processes have been applied to aluminum, lead, plutonium, beryllium, niobium, titanium, vanadium, zirconium, tungsten, molybdenum, uranium, tin and antimony. However, only the non-aqueous refining of aluminum has reached extensive commercial use [17].

The backbone of electrorefining is electrolysis, the use of an external direct current to drive an otherwise non-spontaneous reaction [18, 19]. In its simplest form, an anode of impure metal and a cathode are placed in an electrolytic solution. An electric potential is applied between the anode and cathode driving the impure metal to oxidize, or lose electrons, and become an ion. As an ion is added to the solution from the anode, an ion is simultaneously removed from the solution and deposited on the cathode [4]. When the system consists solely of a metal in a solution of the metal's ions the process is known as electrodeposition [20]. This simple electrolytic conversion of impure metal to pure metal eliminates the many processing steps required for chemical processing and electrorefined metal is purer than that produced by chemical conversion of compounds to metal [17].

The redox potential is the potential at which this process occurs. For active metals, such as uranium, the redox potential is higher than that of water's. This means that if active metals are electrolyzed in an aqueous solution, the water would oxidize preferentially. To prevent this, a non-aqueous treatment, such as in molten salt, is required [18].

The electrolyte in the solution serves as the intermediary between the anode and cathode through the facilitation of the electrotransport of the metal's ions [4]. The electric potential applied drives the atoms in the anode to oxidize and the atoms in the electrolyte to reduce.

This process can be represented by the oxidation reaction



and the reduction reaction



where M is a metal with valency z . Equations II.1 and II.2 are often combined and presented as



Equation II.1 represents the transfer of the metal M from the anode to the solution while Equation II.2 represents the transfer of the metal's ions, M^{z+} , from the solution to the cathode. Thus the

combination of these equations results in the transfer of M from anode to cathode [20]. The presence of the metal's ions and the application of the correct potential between the anode and cathode selectively transports the metal from the anode to the cathode, leaving the impurities behind.

The potential required to drive this reaction is governed by the Nernst Equation

$$E_{\text{cell}} = E_{\text{cell}}^0 + \frac{RT}{zF} \ln Q_r$$

where E_{cell} is the cell voltage, E_{cell}^0 the standard cell potential, R is the gas constant, F is Faraday's constant and Q_r the reaction quotient [20]. For electrodeposition, Q_r simplifies to the activity of the metal's ion, $[M^{z+}]$. The Nernst Equation is then

$$E_{\text{cell}} = E_{\text{cell}}^0 + \frac{RT}{zF} \ln[M^{z+}].$$

At low concentrations, the chemical activity of a species can be approximated by its concentration in mol/L. At higher concentrations ion-ion interactions skew this relationship [20].

In the case where uranium is the electrodeposited metal and UCl_3 the electrolyte, U and UCl_3 oxidize and reduce according to the following chemical half-reactions:



When the half-reactions are combined the ionic equation is



Equation II.6 shows that UCl_3 is not consumed by the reaction and its concentration in the solution remains constant [18].

Faraday's Laws of Electrolysis

The mass of the substance liberated at the anode is governed by Faraday's Laws of Electrolysis. Faraday's first law is

$$m = \left(\frac{Q}{F}\right) \left(\frac{M}{z}\right) \quad (\text{II.7})$$

where Q is the total electric charge passed between the anode and cathode, $F = 96485 \text{ C mol}^{-1}$ is the Faraday constant, M is the molar mass of the substance, z is the valency number of ions of the substance and m the mass of the substance liberated [18]. The total charge passed can be found by integrating the current over the time of the experiment. In other words,

$$Q = \int_0^t I(\tau) d\tau \quad (\text{II.8})$$

where $I(\tau)$ is the time-dependent current measured during the experiment and t the length of the experiment. Combining Equations II.7 and II.8 yields

$$m = \left(\frac{\int_0^t I(\tau) d\tau}{F}\right) \left(\frac{M}{z}\right). \quad (\text{II.9})$$

For DU, $M \approx 238$. Equations II.4 – II.6 show that $z = 3$ when UCl_3 is the electrolyte. Thus for uranium electrolyzed in a solution with UCl_3 Equation II.9 reduces to

$$m = 1.250 \times 10^{-3} \int_0^t d\tau I(\tau). \quad (\text{II.10})$$

Equation II.10 can be used to determine the amount of mass transferred from the anode to cathode. When the transferred mass is equal to the initial mass of uranium, the refining process is complete [21].

The value of m given in Equation II.10 is the theoretical amount of mass transferred from anode to cathode. Actual values are expected to be lower due to Faradaic losses such as chemical byproducts and heat production.

In addition, chemical irreversibilities result in overpotential, the difference between the thermodynamically expected reduction potential and the potential at which the reduction actually occurs. Due to overpotential, more energy is required to drive the reaction than is thermodynamically calculated. This energy difference is manifested as heat. High overpotentials result in a lower collection of mass as more energy is wasted on the production of heat. The magnitude of overpotential present in a system is dependent on the cell design and operating conditions [18].

A common measure of these losses in an electrolytic cell is current efficiency (CE), the ratio of the actual mass collected to the theoretical mass expected from Equation II.10. CE values are close to 100% for copper and nickel plating however, a typical value for chrome plating is 20%. CE depends in general on cell parameters such as the choice of electrolyte, agitation and current density [20].

Mass transport and limiting current

The transport of ions to the electrode occurs in three ways: diffusion, convection and migration [22]. Diffusion and migration are molecular motion due to a concentration gradient and an electric gradient respectively. Convection is molecular motion due to bulk motion of the medium [23].

The concentration gradient arises from the depletion of ions surrounding the electrode. This phenomenon is plotted in Figure II.3. As the current density increases the rapid depletion of ions surrounding the electrode occurs and the concentration gradient increases. At a sufficiently high current, known as the limiting current, the concentration of the ion at the electrode is zero and the rate of reaction is controlled by the rate of mass transport to the electrode [24]. Raising the current beyond the limiting current increases the electrode potential until the potential is high enough to cause another reaction to occur [20].

The dominance of diffusion in this regime makes Fick's Law of diffusion the governing equation. For negligible ion motion from migration and convection, solving Fick's Law with the limiting current condition of zero ion concentration at the electrode yields

$$i_L = \frac{zFDC}{\delta}$$

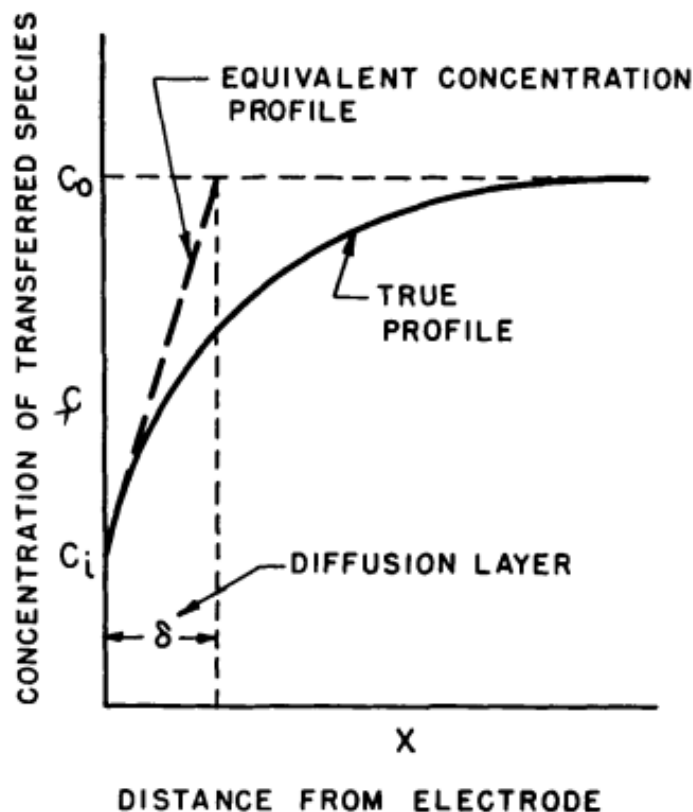


Fig. II.3.: A plot of the concentration gradient versus distance from electrode. The concentration of ions greatly decreases in the direct vicinity of the electrode [22].

where i_L is the limiting current, z the valency number of the ion, D the diffusion coefficient of the ion in the solution, C the concentration of the ion in the solution and δ the boundary layer thickness [24]. Factoring in convection and migration greatly complicates the derivation of the limiting current.¹

In mass transport controlled reactions, increasing the mass transport to the electrode increases the rate of reaction. Thus, current density and agitation affect the rate of reaction. Operating near the limiting current maximizes mass transport by diffusion through maximizing the concentration gradient while adding agitation increases convection through the boundary layer [22].

¹Equations for the limiting current where mass transport due to convection is not negligible are provided in [22].

CHAPTER III

LITERATURE REVIEW

Los Alamos National Laboratory

In 1958, Los Alamos National Laboratory (LANL) developed a non-aqueous, pyrometallurgical refining process to recover and purify plutonium from scrap and aged weapons-grade plutonium [25]. This process is the historical basis for later experiments conducted by Argonne National Laboratory (ANL) and Idaho National Laboratory (INL). From 1964–1977, approximately 1,568 kg of plutonium metal greater than 99.95% pure was produced in 653 runs from 1,930 kg of metal fabrication scrap [17]. Figure III.1 shows LANL’s electrorefiner (ER) design. The system used an equimolar mixture of NaCl-KCl as the molten salt solvent for its notable properties of non-hygroscopy and a melting point of 650 °C.

Two types of plutonium electrolyte were tested:

1. Plutonium halide salts (PuCl_3 , PuF_3 or PuF_4)
2. Electrolytic generation of PuCl_3

In option 1, PuCl_3 and PuF_3 were directly used as the electrofacilitator of plutonium ions to the cathode while PuF_4 was reduced to PuF_3 before the electrorefining step according to the following equation



Option 2 was used to purify small amounts of plutonium of unusual isotopic composition. In this case, the reduction of Pu^{+3} to metal competes with the reduction of Na^+ but does not require initial addition of electrolyte. Option 2 uses the following reactions



Ceramic crucibles, tungsten cathodes and MgO stirrers were used [17].

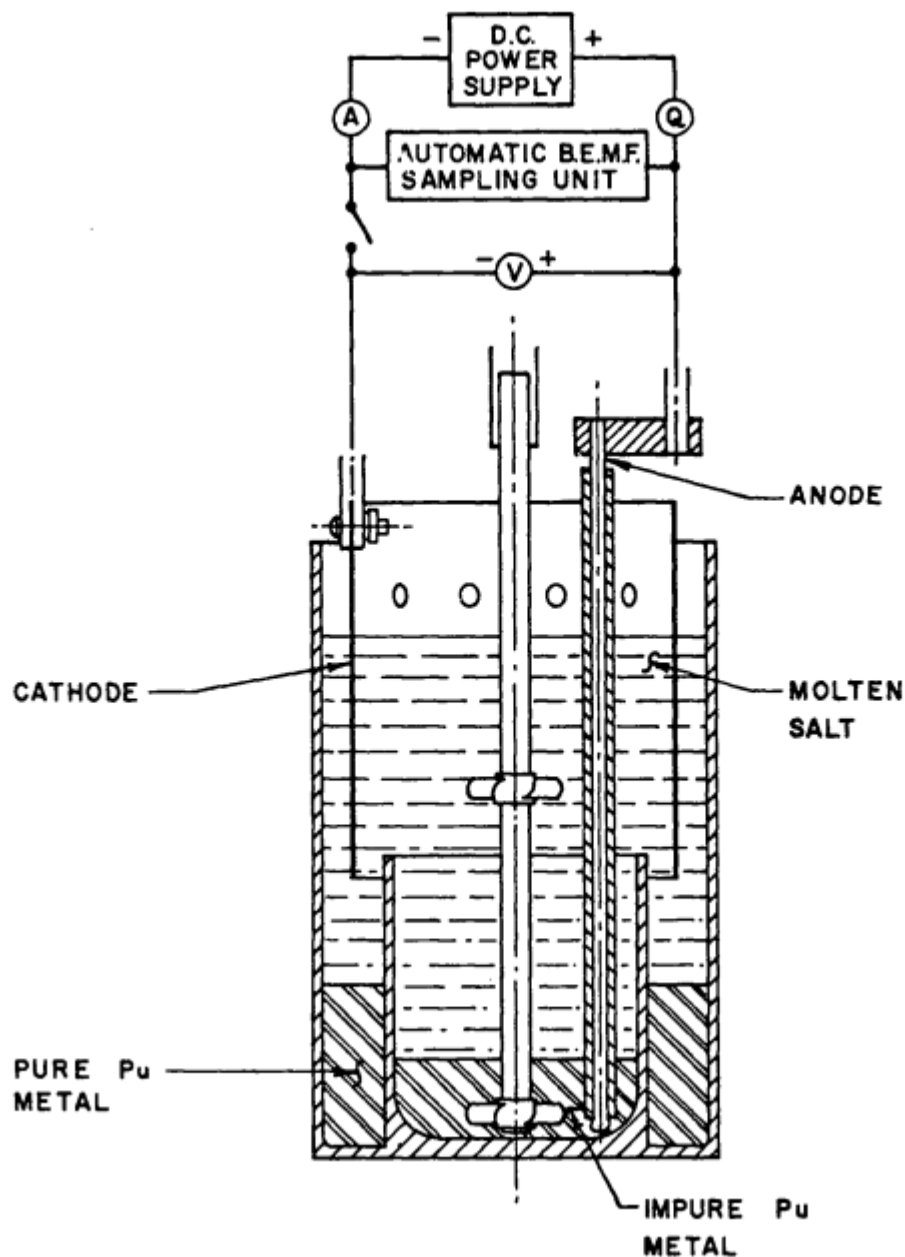


Fig. III.1.: A schematic drawing of LANL's electrorefiner design [17].

Argonne National Laboratory

Initial design

In 1986, Leslie Burris, Robert Steunenberg and Bill Miller at ANL applied electrorefining to the metal fuel discharged from the Integral Fast Reactor (IFR) prototype Experimental Breeder Reactor

II (EBR-II) [4, 21]. The focus of the project was to extract plutonium and uranium from the core and blanket materials, remove fission products from the core and blanket materials and dispose of the waste. The extracted plutonium and uranium was then re-enriched for reuse in the EBR-II. The removal of fission products from the recycled fuel prompted a switch to a fuel alloy consisting of plutonium, zirconium and uranium and a blanket alloy of uranium and zirconium [26]. Thus early stages of electrorefining at ANL focused on the recovery of plutonium and uranium and the retention of zirconium.

The uranium and plutonium were refined in a LiCl-KCl eutectic solution with approximately 10 wt% UCl_3 [4, 21]. An applied potential oxidized the uranium and plutonium to their chlorides as an equal amount of uranium was deposited on the cathode [27].

A cadmium bottom layer was introduced into the design of the ER to separate the fuel elements from the stainless-steel cladding. The fuel elements are soluble in liquid cadmium, but the stainless steel cladding is not. The fuel elements dissolved into the solution leaving the cladding behind. The process of dissolving the fuel in the cadmium bottom layer is known as direct dissolution. This is opposed to anodic dissolution where the fuel is suspended in the molten salt solution and electrochemically dissolved [28].

Direct dissolution required much more time than anodic dissolution, prompting a change to anodic dissolution. This process proved to be successful with high uranium recoveries of over 99% [27].

Codeposition of uranium and plutonium was achieved by using a solid cathode for collecting uranium and a liquid cadmium cathode for collecting plutonium. The alkali, alkaline earth and rare-earth metals were oxidized to their chlorides and remained in the molten salt solution. Noble metal fission products either remained in the basket or fell into the cadmium bottom layer. However, when the refining project moved to large-scale designs only the deposition of uranium was considered [27].

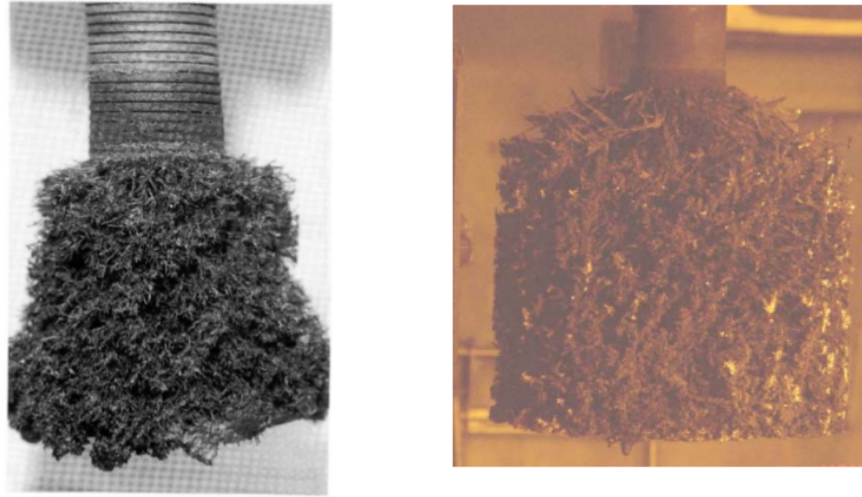


Fig. III.2.: Pictures of the dendritic growth of uranium cathode deposits. The thin dendrites have an unstable, low density structure and often fall off the cathode [29, 30].

Engineering scale design

The switch from lab scale to engineering scale resulted in a shift from codeposition to the collection of uranium only. Despite this shift, the cadmium bottom layer remained in the design of the engineering scale refiner.

The uranium cathode deposits grew in an unstable, dendritic structure that expanded radially outward. Dendrites often fell off the cathode or needed to be scraped off when the growth extended to the refiner wall. This loss of deposited uranium greatly reduced current efficiency. The cadmium layer served as a collection pool where fallen uranium dendrites and noble metal particulates were collected and dissolved. The dissolved uranium was recovered from the cadmium layer with an electrorefining process where the cadmium pool was the anode [21]. A schematic drawing of the ER design is presented in Figure III.3.

Newer anode designs used Fuel Dissolution Baskets (FDBs) (Figure III.4) to hold the chopped SNF in the molten salt solution. This cruciform design implemented a mesh of stainless steel to allow the transport of uranium while retaining noble metal particulates [21, 27].

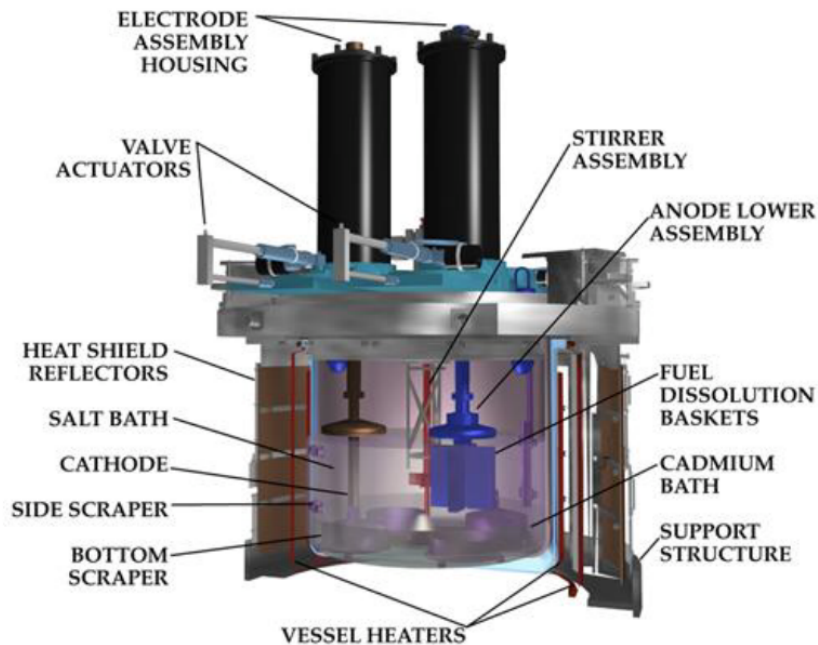


Fig. III.3.: A schematic drawing of ANL's ER design. This design incorporated a cadmium bottom layer to catch fallen uranium dendrites and noble metal particulates. Side and bottom scrapers contained the radial growth from the dendritic structure of the uranium deposit on the cathode [21].

The power supply, which supplied the potential between the anode and cathode, was operated in controlled current mode. The applied voltage was maintained above the redox potential of uranium but below a cut-off potential defined by the potential required for undesirable reactions such as the dissolution of zirconium to occur. As the redox reaction progressed, the amount of uranium in the FDBs decreased causing an increase in anode resistance and cell voltage. The current was varied to maintain the cell voltage in the desirable range. The refining process was deemed complete when the theoretical quantity of charge had passed or the anode resistance became so high that a current of 12 A could not be maintained without surpassing the cut-off voltage [21].

Further experiments on the collection of uranium proved that direct dissolution in liquid cadmium was not necessary. Current efficiencies of 50% were achieved along with 99.8% of the fuel being removed from the cladding. In addition, cadmium aerosols were found to diffuse through the LiCl-KCl solution and deposit on the glove box windows and equipment. Cadmium is extremely toxic

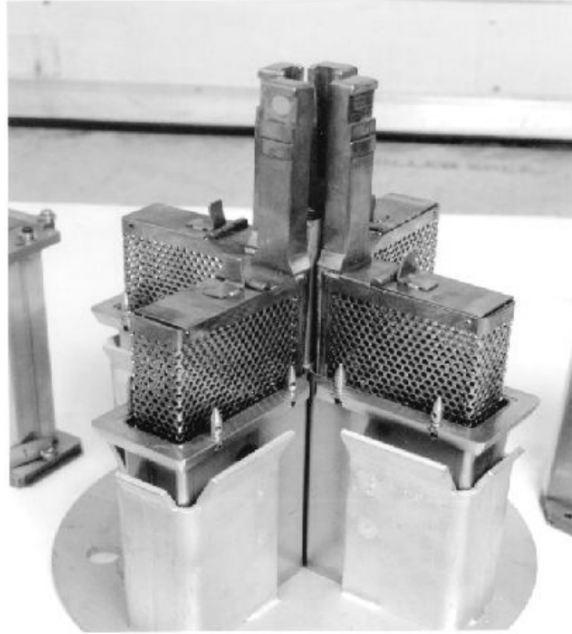


Fig. III.4.: A picture of the Fuel Dissolution Baskets used in ANL's electrorefiner. The stainless steel mesh allowed the electrotransported uranium to leave the FDBs while helping to retain noble metals [21].

and thus cadmium releases from the ER were not tolerated. Cover gas purifiers were employed to remove the cadmium from the glove box. However, the use of the cadmium bottom layer was eventually discontinued [27].

Advanced designs

The primary difference between the engineering scale design and the advanced design was the elimination of the cadmium pool to avoid the problems associated with cadmium vaporization and condensation in the glove box. The removal of the cadmium bottom layer, which served to absorb and dissolve fallen noble metal fission product particulates, prompted the addition of a filtration system to remove the escaped particulates from the electrolyte.

Figure III.5 shows a drawing of the advanced design. The noble metal particulates that fall out of the anode basket are added to the solution along with the rare earth metals. The cladding hulls

remained in the anode basket. The contaminated salt required filtration to remove rare earth and noble metals. The contaminants were then stored in zeolite [27].

The focus also shifted to higher throughput refiners with large batch sizes of 100 kg of initial fuel and a refining rate of 40 kg U/hour. This design consisted of 20 stainless steel anode baskets shown in Figure III.6.

At this point ANL expanded from EBR-II fuel to work with spent fuels from other reactors such as the Hanford "N" Reactor and Oak Ridge National Laboratory's Molten Salt Reactor Experiment (MSRE). The Hanford "N" Reactor used a metal fuel similar to the EBR-II's spent fuel eliciting only minor changes to the ER design. However, the aluminum-based fuel used in the MSRE required significant alterations due to the decomposition of the salt from the high energy gamma rays emitted from ^{208}Tl .

The ER project expanded further into the processing of spent oxide fuels with the intent of preparing the fuel for safe disposal [27].

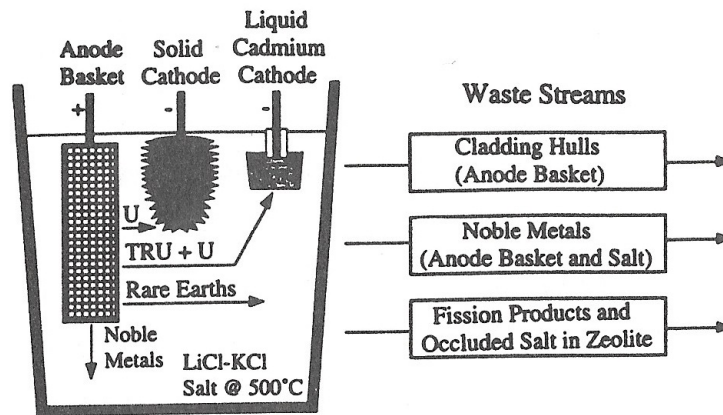


Fig. III.5.: A drawing of the advanced ER design. The cadmium bottom layer was eliminated in this design. The drawing shows the transport locations for uranium, rare earths and noble metals [27].

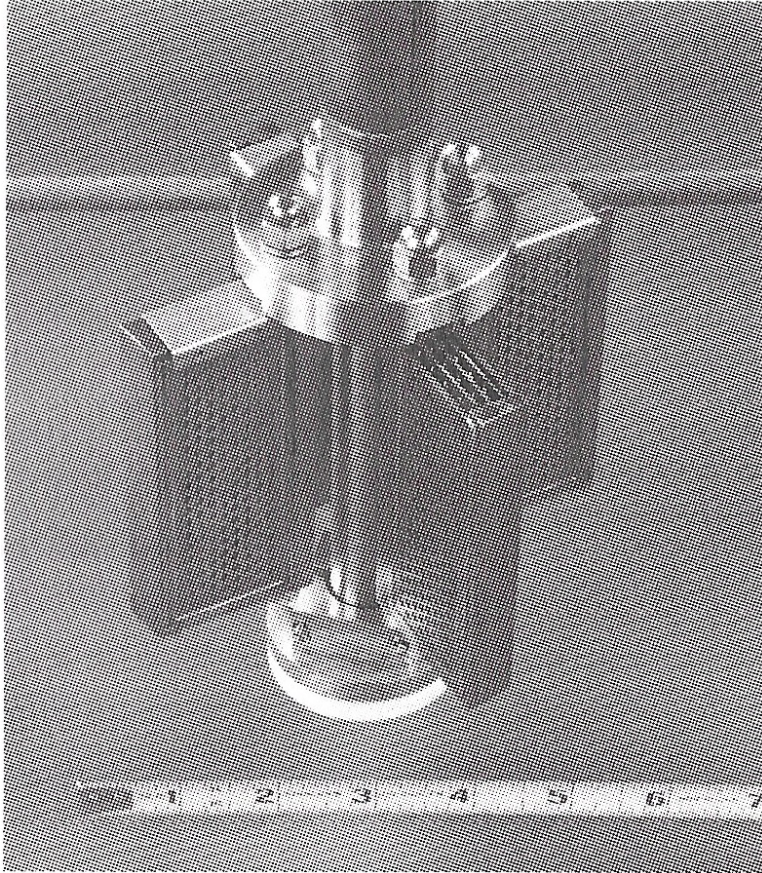


Fig. III.6.: A picture of an FDB from a high throughput design ER constructed in 1995 at Argonne National Laboratory [27].

Idaho National Laboratory

INL continued ANL's work on the engineering scale ER with a focus on improving current efficiency. CE was greatly lowered by the loss of mass due to fallen uranium dendrites. INL reports that CE was improved from 50% to 65-76% by salt agitation. The refiner agitated the molten salt by rotating the anode and cathode. Agitation helped to increase diffusive mass transfer resulting in a denser, more stable cathodic deposit that was more likely to stay on the cathode. Higher mass transport and a more stable deposit structure resulted in minimal loss of uranium to the cadmium layer and a higher current efficiency [30].

INL also conducted experiments on the impact of interrupting current on the anodic process using ANL's engineering scale ER. In these experiments external current was applied between the FDBs

and cathode for 6 seconds. The FDBs were then electrically disconnected as the cadmium bottom layer was connected as the anode for 2 seconds. This cycle supplied a 2 second relaxation period inside the FDBs. It was observed that the average anodic resistance was consistently lower than experiments conducted with continuous current. Higher zirconium and noble metal retention was reported [31].

CHAPTER IV

EXPERIMENTAL SETUP

Glove box

Uranium is a pyrophoric metal and can combust when uranium powder is exposed to the oxygen in the air. Oxidation of uranium samples reduces the purity of the sample in addition to the possibility of combustion. To prevent the oxidation of the depleted uranium samples, all experiments will be conducted in the argon filled glove box shown in Figure IV.1. The use of a dry, inert environment will also prevent the salt from forming hydrates with water in the air and help keep the salt as pure as possible.

A Photohelic pressure gage maintains the glove box at a pressure slightly above atmospheric pressure. The higher pressure inside forces argon out of any leaks, preventing air from leaking in and reducing the purity of the argon environment. Operating at positive net pressures has the disadvantage that a catastrophic leak has the potential to push material out into the lab. Other glove box designs prevent this by operating under a slight vacuum. In this case, the outside environment is pulled in by the pressure difference. This serves to keep dangerous materials inside the glove box in the event of a catastrophic leak but also makes minimizing the oxygen content much more difficult as any leaks will pull oxygen into the system.



Fig. IV.1.: A picture of the glove box at the Fuel Cycle and Materials Laboratory, Texas A&M University.

With a half-life of 4.5 billion years, ^{238}U , the primary component of DU, has a low activity. Factoring in decays from daughter products of the uranium series does add beta and gamma emissions in addition to the alpha particles emitted by ^{238}U . However, the total activity remains low. In addition, only small amounts of solid DU will be used. Therefore, electrorefiner experiments do not necessitate the added costs and difficulties of maintaining a negative pressure glove box.

The Photohelic pressure gauge is programmed in set point mode where a single pressure setting is used. When the inside pressure drops below the set point, argon is added until the pressure exceeds the set point. Due to the small volume of the glove box, using the glove box causes a sharp increase in pressure as the volume of the gloves is pushed inside. The system handles overpressure situations such as this through multiple oil filled manometers that are calibrated to vent at sufficiently high pressures.

Materials can be added to the glove box from either of its two ports. Each port has an outer and inner door. To prevent diluting the argon environment, the inner doors are not opened until the outside environment is removed from the ports. This is accomplished by flooding the port with a continuous stream of argon to purge the air from the port or a combination of purging and vacuuming the port. The right port is purge only while the left port has a vacuum line and can be both purged and evacuated. In addition, the left port has a water cooled furnace and vacuum tight doors.

This glove box suffered severe water damage in storage and many of the vacuum line components were unusable. In addition, the presence of large leaks in the side panels and argon lines prevented the glove box from maintaining pressure. In preparation for this experiment, the glove box was overhauled with new vacuum and argon lines and completely resealed in an effort to minimize leaks.

Maintenance of any high purity environment in a glove box is a difficult task due to the large number of leak locations. The initial condition of the glove box has expounded these difficulties and the purity of the glove box environment has become a major design consideration.

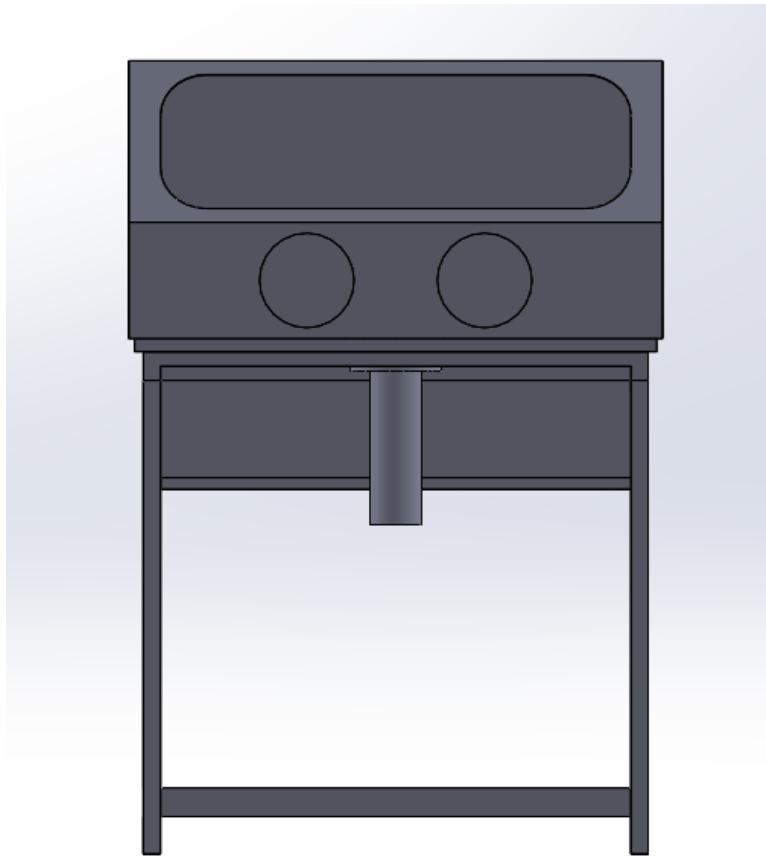


Fig. IV.2.: A Solidworks drawing of the heater well system hanging below the glove box. The heater well will be connected through the floor of the glove box.

Heater well

Electrorefining experiments will be conducted in a heater well attached to the bottom floor of the glove box shown in Figure IV.2. Using a heater well is necessary to free up room inside the glove box and to modularize the refiner system into the inner vessel and refiner vessel shown in Figure IV.3. The refiner vessel houses the experiment while the inner vessel serves as the connection point between the glove box and the refiner vessel.

Refiner vessel

The refiner vessel has a 4 inch inner diameter, is 20 inches tall and is made of quarter inch stainless steel. A 250 mL stainless steel crucible will be placed on a layer of insulation on the bottom of the

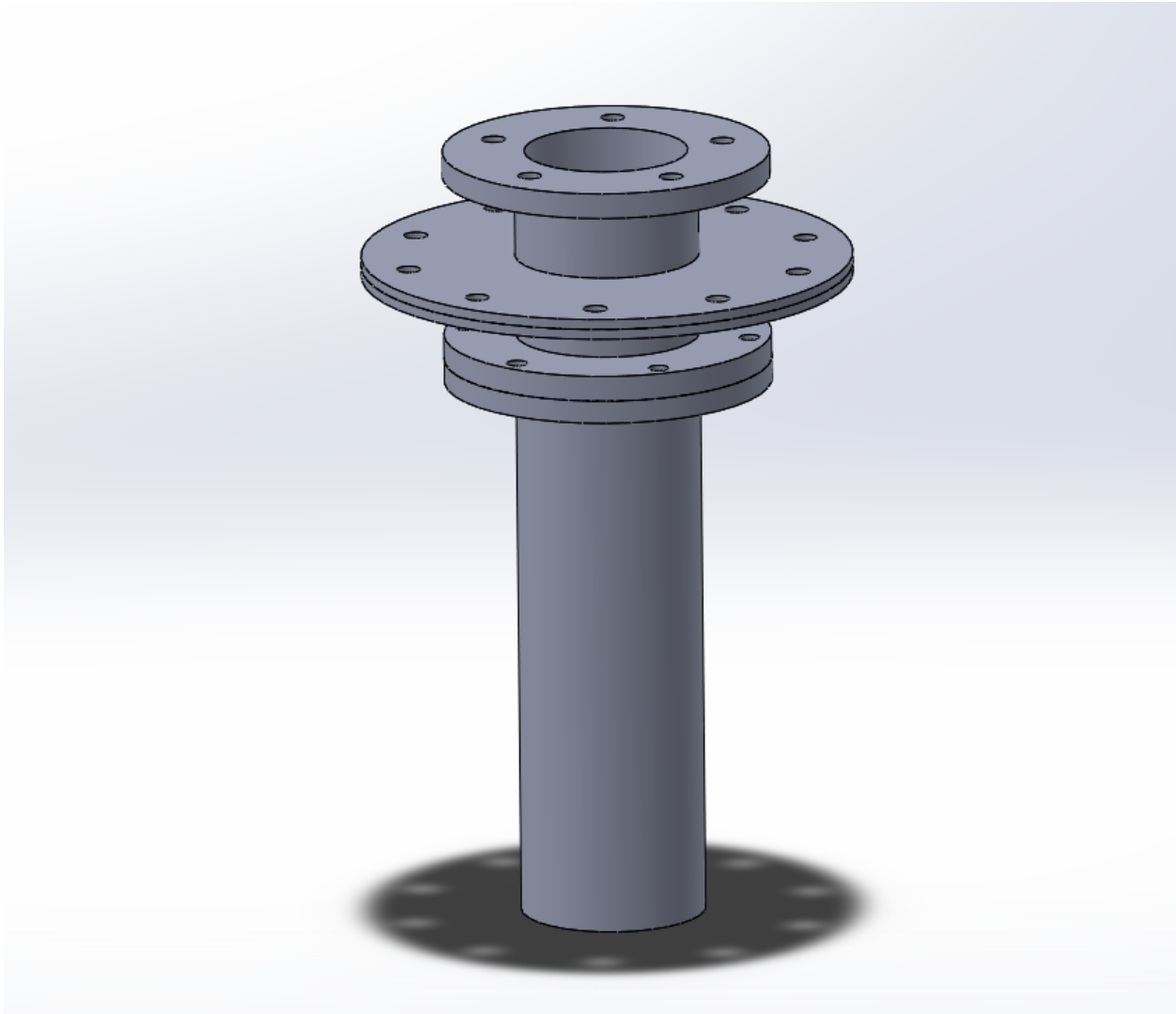


Fig. IV.3.: A side view of the heater well system consisting of the inner vessel and refiner vessel.

refiner vessel. The layer of insulation will raise the crucible to the correct height within the vessel. The stainless steel crucible serves as the container for the electrorefining process.

A cylindrical, 4.5 inch inner diameter, Watlow, ceramic fiber, high temperature heater will be placed around the outside of the refiner vessel as shown in Figure IV.4. The heater's 6 inch height will provide even heating to the entire crucible.

Placing the heater outside the refiner vessel increases the modularity of the system. In the case of failure the heater can be removed or debugged without dismantling the system and risking introducing oxygen to the glove box environment. External placement of the heater will reduce

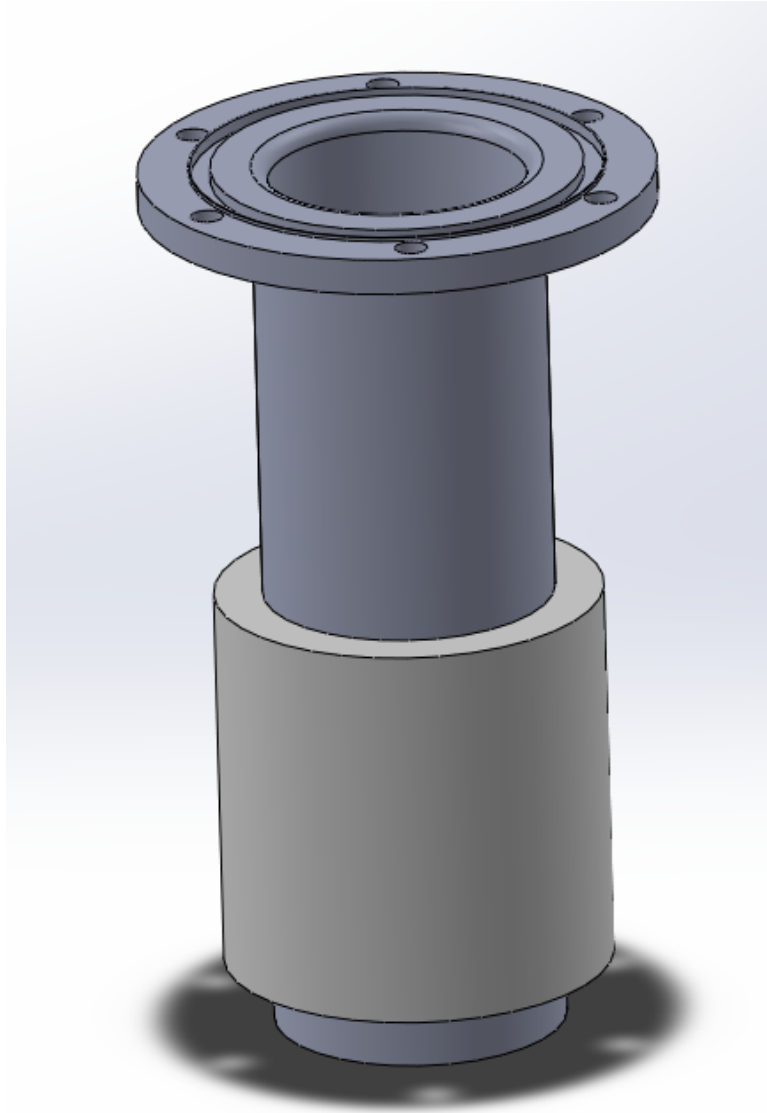


Fig. IV.4.: A Solidworks drawing of the refiner vessel and Watlow ceramic fiber heater.

heating efficiency as some of the energy will go to heating the vessel. This may increase the time required to reach the desired temperature. The ceramic fiber heater's maximum temperature of 1200 °C is over a factor of 2 higher than the desired operating temperature of 500 °C and will not hinder the experiment.

Just below the flange, copper cooling jackets and a vent have been installed (see Figure IV.5). A chiller will be connected to the cooling jackets to provide water cooling to the vessel head to lower



Fig. IV.5.: A picture of the refiner vessel's copper cooling jackets and vent.

the temperature felt by the operator and to keep the rubber gasket used to connect the refiner vessel to the inner vessel within its temperature limits.

To maintain the modularity of the system, the refiner vessel's unorthodox, custom made flange will be machined to match the flat faced flange of the inner vessel.

Inner vessel

The inner vessel (Figure IV.6) is a doubly flanged cylinder made of quarter inch stainless steel with an inner diameter of 4 inches. A quarter inch stainless steel, sealing disk with a 15 inch diameter will be welded around the middle of the inner vessel. A quarter inch stainless steel support disk (shown in Figure IV.7) of the same outer diameter but with a larger inner diameter of 12 inches will serve as a support disk to prevent damaging the glove box floor. The support disk has an inner diameter large enough to be able to fit around the inner vessel's lower flange.

A square hole with side length 9 inches will be cut into the glove box floor. The hole is large enough for the inner vessel to fit through except for the 15 inch sealing disk. The inner vessel will be placed inside the glove box and lowered down through the hole until it rests on the sealing disk. The support disk will then be placed underneath the sealing disk, sandwiching the glove box floor between the two disks. Matching holes will be drilled on the outer perimeter of the disks through both disks and the glove box floor. The inner vessel will then be attached with nuts and bolts and

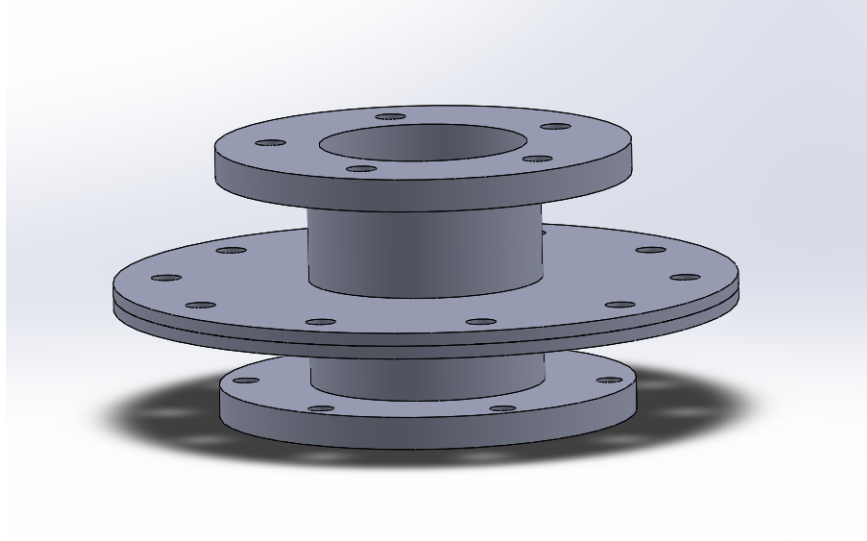


Fig. IV.6.: A Solidworks drawing of the inner vessel system.

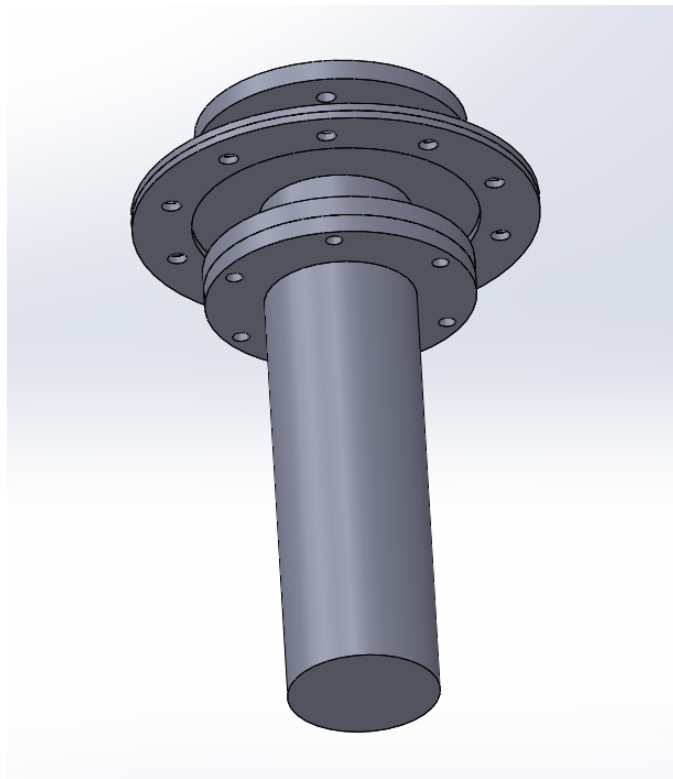


Fig. IV.7.: A bottom view of the heater well system highlighting the size of the inner diameter of the support disk. The large inner diameter allows the support disk to fit over the refiner vessel's flange.

sealed with silicone to minimize leaks. The refiner vessel can then be attached to the glove box by connecting to the matched flange of the inner vessel.

By capping the upper flange with a blank flange, the refiner vessel can be removed without affecting the purity of the glove box. This modularity will allow for other experiments to attach to the inner vessel with ease.

A jack will be attached from the ground to the bottom of the refiner vessel to alleviate the added stress on the glove box floor from the weight of the heater well system.

Refiner crucible

The molten LiCl-KCl, anode, cathode and reference electrode will be housed in a 250 mL stainless steel crucible located in the refiner vessel. A drawing of the crucible is provided in Figure IV.8. The crucible will be raised to the heater's active area by placing it on a layer of insulation.

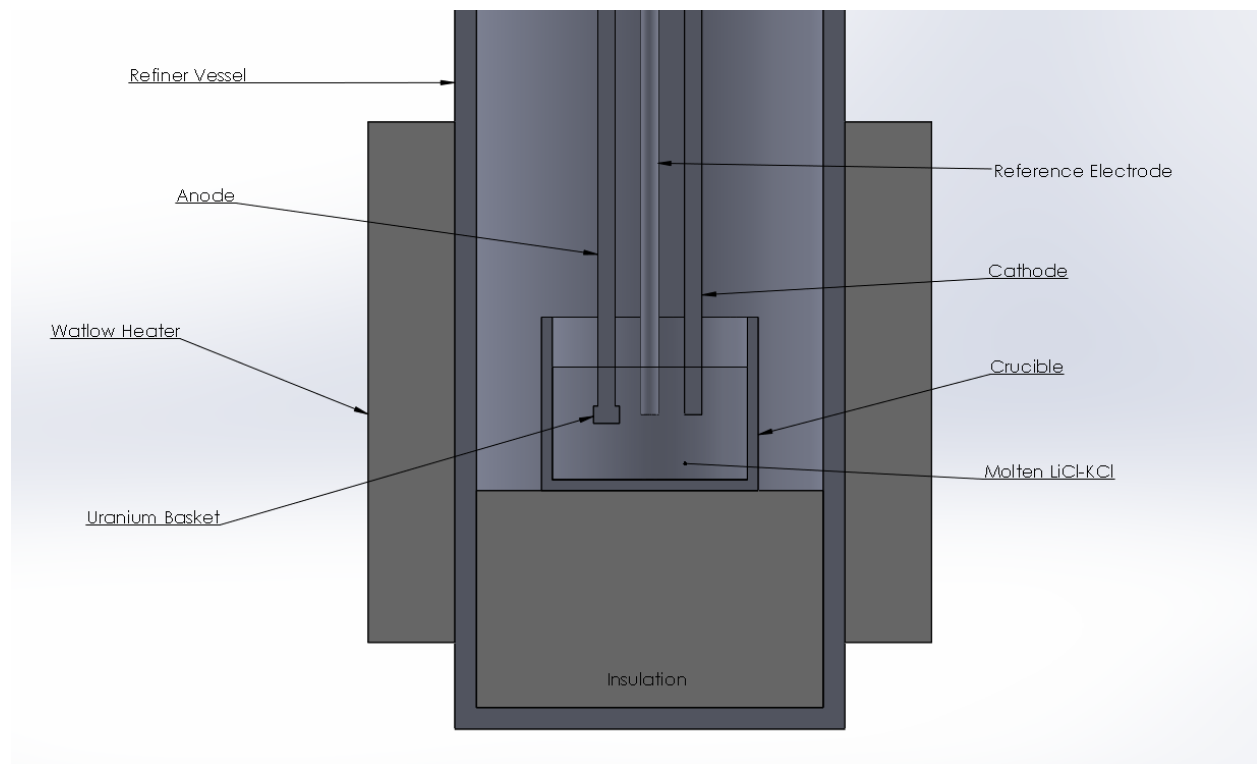


Fig. IV.8.: A Solidworks drawing of the refiner crucible located in the refiner vessel showing the placements of the crucible, anode, cathode, reference electrode and uranium basket.

The stainless steel anode, molybdenum cathode and Ag/AgCl reference electrode will be lowered through the inner and refiner vessels into the molten salt and will be held in place by a scaffolding system inside the glove box. A small, 100 cm³ basket will be connected to the anode and will suspend the impure uranium samples in the molten salt.

The anode and cathode will be connected to a power supply placed outside of the glove box.

Electrorefining process

A eutectic solution of LiCl-KCl-UCl₃ will be heated using the Watlow ceramic fiber heater to 500 °C in the heater well of the glove box. A process controller will maintain the salt at the refiner operating temperature. Uranium samples will be loaded into the glove box through one of its ports and placed in the uranium basket on the anode. The anode/uranium basket, cathode and reference electrode will be lowered into the molten salt and secured into the scaffold system inside the glove box.

The power supply will be turned and on and set to deliver a high amperage, low voltage current between the anode and cathode. Using the potential from the reference electrode, a process control program will regulate the outputted current to maintain the voltage above the redox potential of uranium and below the redox potential of LiCl-KCl. Once the theoretical quantity of mass has transferred, the power supply will be turned off.

CHAPTER V

LIST OF DEVICES

- Glove box
- Power supply
- Watlow Ceramic Fiber Heater
- Temperature process controller
- Stainless steel crucible
- Stainless steel anode
- Molybdenum cathode
- Stainless steel uranium basket
- Ag/AgCl reference electrode
- Vacuum pump
- Chiller
- Photohelic Pressure Gauge
- Thermocouples
- Support jack

CHAPTER VI

FUTURE WORK

The designs shown in this thesis serve as the basis for a simple electrorefiner. There are several functionalities to add to the refiner system and many points of investigation for future research.

Due to the astronomical cost of high purity LiCl-KCl eutectic and the sparse availability of UCl_3 , a method for the creation of the LiCl-KCl- UCl_3 eutectic solution is required. The LiCl-KCl eutectic solution can be produced by combining the correct ratios of the constituent salts, LiCl and KCl. However, the production of UCl_3 presents a more difficult problem. A possible method involves reacting U with CdCl_2 in the LiCl-KCl solution to produce LiCl-KCl- UCl_3 . The eutectic solution will then need to be removed by distilling and collecting the chloride salts. The financial feasibility and practicality of this method will be investigated in addition to streamlined ways of integrating the production of UCl_3 into electrorefining experiments.

A possible modification to the refiner system is the use of a sophisticated process control program. This program could employ the theoretical mass equations presented earlier and cut-off voltages to autonomously conduct refiner experiments.

Salt agitators could be added to the refiner crucible to facilitate the diffusion and electrotransport of uranium ions. This could be accomplished through a rotating anode and cathode system or through the addition of a magnetic stirrer beneath the crucible. A simple experiment of varying the revolution speed and amount of agitation could be conducted to verify the experimental results of INL.

A recirculation system using oxygen and hydrogen sensors and a zeolite bed to trap oxygen and water could also be added to the glove box to decrease oxygen and hydrogen contamination.

Lastly, a method of removing the molten salt from the cathode deposits is required to be able to check the purity of the refined uranium.

REFERENCES

- [1] World Nuclear Association, Processing of Used Nuclear Fuel, <http://www.world-nuclear.org/info/nuclear-fuel-cycle/fuel-recycling/processing-of-used-nuclear-fuel/>.
- [2] M. F. Simpson, *Nuclear Fuel Reprocessing*.
- [3] T. Todd, Spent Nuclear Fuel Reprocessing, **2008**, http://www.state.nv.us/nucwaste/library/Reprocessing/NRCseminarreprocessing_Terry_Todd.pdf.
- [4] L. Burris, R. K. Steunenbergh, W.E. Miller, “The Application of Electrorefining for Recovery and Purification of Fuel Discharged from the Integral Fast Reactor”, **1986**.
- [5] W. H. Hannum, Smarter Use of Nuclear Waste.
- [6] L. Lerner, **2012**, <http://www.anl.gov/articles/nuclear-fuel-recycling-could-offer-plentiful-energy>.
- [7] L. R. Morss, *The Chemistry of the Actinide and Transactinide Elements*.
- [8] N. Holden, *Isotopic Composition of the Elements and Their Variation in Nature – A Preliminary Report*, **1977**.
- [9] I. A. E. Agency, *Analytical Methodology for the Determination of Radium Isotopes in Environmental Samples*, **2010**.
- [10] M. A. McDiarmid, “Depleted Uranium and Public Health”, **2001**.
- [11] J. E. Turner, *Atoms, Radiation and Radiation Protection*, **2007**.
- [12] Oak Ridge Institute for Science and Education, “Radiological and Chemical Properties of Uranium”.
- [13] R. M. Mayo, *Nuclear Concepts for Engineers*, **2001**.
- [14] E. I. Hamilton, *Applied Geochronology*, **1965**.
- [15] S. Keith, *Toxicological Profile for Uranium*.
- [16] Los Alamos National Laboratory, Uranium, <http://periodic.lanl.gov/92.shtml>.
- [17] L. J Mullins, *A Review of Operating Experience at the Los Alamos Plutonium Electrorefining Facility*.
- [18] A. J. Bard, *Electrochemical Methods*.

- [19] Brown, LeMay, Bursten, *Chemistry: The Central Science*, **2014**.
- [20] M. Paunovic, *Fundamentals of Electrodeposition*, **2006**.
- [21] S. X. Li, T. A. Johnson, D. V. Laug, “Experimental Observations on Electrorefining Spent Nuclear Fuel in Molten LiCl-KCl/Liquid Cadmium System”, **1999**.
- [22] C. W. Tobias, “Diffusion and Convection in Electrolysis – A Theoretical Overview”.
- [23] A. W. Bott, “Mass Transport”, **1996**.
- [24] R. V. Kumar, *An Introduction to Electrochemical Cells*.
- [25] R. Baker, J. Leary, *Recent Developments in Plutonium Processing in the United States*.
- [26] J. Battles, “Pyrometallurgical Processes for Recovery of Actinide Elements”.
- [27] R. K. Steunenberg, *From Test Tube to Pilot Plant*.
- [28] J. Willit, “Electrorefining Uranium and Plutonium - A Literature Review”.
- [29] Tadafumi Koyama, Masatoshi Iizuka, Yuichi Shoji, Reiko Fujita, “An Experimental Study of Molten Salt Electrorefining of Uranium Using Solid Iron Cathode and Liquid Cadmium Cathode for Development of Pyrometallurgical Reprocessing”, **1996**.
- [30] Shelly X. Li, Thomas A. Johnson, Brian R. Westphal, Kenneth M. Goff, Robert W. Benedic, “Electrorefining Experience for Pyrochemical Processing of Spent EBR-II Driver Fuel”, **2005**.
- [31] S. X. Li, “Anodic Process of Electrorefining Spent Nuclear Fuel in Molten LiCl-KCl- UCl_3 /Cd System”, **2002**.